Received: 16 July 2017 | Accepted: 31 March 2018

DOI: 10.1111/gbi.12289

ORIGINAL ARTICLE

WILEY gebiology

# Tracking the rise of eukaryotes to ecological dominance with zinc isotopes

Terry T. Isson[1] | Gordon D. Love[2] | Christopher L. Dupont[3] | Christopher T. Reinhard[4] | Alex J. Zumberge[2] | Dan Asael[1] | Bleuenn Gueguen[5] | John McCrow[6] | Ben C. Gill[7] | Jeremy Owens[8] | Robert H. Rainbird[9] | Alan D. Rooney[1] | Ming-Yu Zhao[1] | Eva E. Stueeken[10] | Kurt O. Konhauser[11] | Seth G. John[12] | Timothy W. Lyons[2] | Noah J. Planavsky[1]

[1]Geology and Geophysics, Yale University, New Haven, Connecticut

[2]Earth Science, University of California, Riverside, Riverside, California

[3]Microbial and Environmental Genomics, J. Craig Venter Institute, San Diego, California

[4]Georgia Institute of Technology, Atlanta, Georgia

[5]Earth Science, Université de Bretagne Occidentale, Brest, France

[6]J. Craig Venter Institute, Rockville, Maryland

[7]Geosciences, Virginia Tech, Blacksburg, Virginia

[8]Florida State University, Tallahassee, Florida

[9]Geology, Geological Survey of Canada, Ottawa, ON, Canada

[10]School of Earth and Environmental Sciences, University of St Andrews, St Andrews, Scotland, UK

[11]Earth and Atmospheric Sciences, University of Alberta, Edmonton, AB, Canada

[12]Earth Science, University of Southern Carolina, Los Angeles, California

**Correspondence**
Terry T. Isson, Yale University, New Haven, CT.
Email: terry.t.isson@gmail.com

**Funding information**
NSF FESD Program; NASA Astrobiology Institute

## Abstract

The biogeochemical cycling of zinc (Zn) is intimately coupled with organic carbon in the ocean. Based on an extensive new sedimentary Zn isotope record across Earth's history, we provide evidence for a fundamental shift in the marine Zn cycle ~800 million years ago. We discuss a wide range of potential drivers for this transition and propose that, within available constraints, a restructuring of marine ecosystems is the most parsimonious explanation for this shift. Using a global isotope mass balance approach, we show that a change in the organic Zn/C ratio is required to account for observed Zn isotope trends through time. Given the higher affinity of eukaryotes for Zn relative to prokaryotes, we suggest that a shift toward a more eukaryote-rich ecosystem could have provided a means of more efficiently sequestering organic-derived Zn. Despite the much earlier appearance of eukaryotes in the microfossil record (~1700 to 1600 million years ago), our data suggest a delayed rise to ecological prominence during the Neoproterozoic, consistent with the currently accepted organic biomarker records.

**KEYWORDS**
carbon cycle, Earth history, eukaryotes, marine productivity, ocean chemistry, zinc, zinc isotopes

  

## 1 | INTRODUCTION

While eukaryotic microalgae are responsible for a substantial portion of marine export production today (Falkowski et al., 2004), primary production and microbial communities in the Archean and Proterozoic oceans are traditionally viewed to have been dominated by unicellular prokaryotes (Brocks et al., 2017; Butterfield, 2015; Knoll, 2014). This long-term shift toward a more eukaryote-rich Earth system has been mechanistically linked to numerous major events in Earth's history, in particular the onset of low-latitude "Snowball Earth" glaciations, major carbon cycle perturbations, and ocean-atmosphere oxygenation during Neoproterozoic time (e.g., Feulner, Hallmann, & Kienert, 2015; Tziperman, Halevy, Johnston, Knoll, & Schrag, 2011; Zhu et al., 2016). However, although it has been commonly proposed that there was a major ecosystem shift during the Neoproterozoic, there are relatively few constraints on either the extent of marine productivity or the composition of plankton communities through most of Earth's history.

Thus far, two main approaches have been applied to track the early evolution of primary producers. The microfossil record has been used both to delineate the appearance of the earliest definitive eukaryotes at ~1700–1600 Ma (Butterfield, 2015; Knoll, Javaux, Hewitt, & Cohen, 2006) and to track the onset of extensive algal primary productivity by ~800 Ma (Brocks et al., 2017; Feulner et al., 2015; Knoll, 2014). Molecular fossils (organic biomarkers) have also been used to track the evolution of phototrophs and the balance of bacterial versus algal productivity. For example, the ratio of hopane (e.g., bacterial) to sterane (e.g., eukaryotic) biomarkers can potentially provide a first-order view of the relative balance between bacterial and eukaryotic inputs in aquatic depositional settings (Figure 1). While there have been numerous reports of abundant eukaryotic biomarkers in Mesoproterozoic rocks (e.g., Zhang et al., 2016), recent lipid biomarker evidence, using clean analytical methodologies to minimize contamination, suggests that the earliest detectable and robust eukaryotic (24-alkylated) sterane biomarkers appear sometime within the Neoproterozoic Era (<1000 Ma) (e.g., Brocks et al., 2015, 2017; French et al., 2015; Love et al., 2009) (see Appendix S1). Earlier reports of abundant steranes, as old as 2700 Ma, are now attributable to contamination artifacts (French et al., 2015). Here, we propose a novel tracer for shifts in marine ecosystem structure—that is, a coupled record of the phase-specific sedimentary enrichment and stable isotope composition of zinc (Zn).

## 2 | THE BIOLOGICAL USE OF ZINC

Stable isotopes of Zn have the potential to track the rise and ecological expansion of eukaryotes in the global ocean. While all organisms utilize Zn, modern eukaryotic phytoplankton appear to have elevated Zn demands and elevated Zn/C ratios relative to cyanobacteria (Nuester, Vogt, Newville, Kustka, & Twining, 2012; Quigg, Irwin, & Finkel, 2011; Twining, Baines, & Fisher, 2004; Twining et al., 2003, 2011). In addition, cultures show that Zn can be colimiting for eukaryotic algae (e.g., Zn-C and Zn-P colimitation) (Brand, Sunda, & Guillard, 1983; John, Geis, Saito, & Boyle, 2007; Morel et al., 1994; Schulz et al., 2004; Shaked, Xu, Leblanc, & Morel, 2006; Sunda & Huntsman, 1992, 1995). Specifically, reduced growth rates have been shown in multiple (>25) eukaryotic phytoplankton species at free $Zn^{2+}$ concentrations below $10^{-11.5}$ M while other more tolerant species only exhibit a decline starting at $10^{-13}$ M (Anderson, Morel, & Guillard, 1978; Brand et al., 1983; Ellwood & Hunter, 2000; John et al., 2007; Morel et al., 1994; Schulz et al., 2004; Shaked et al., 2006; Sunda & Huntsman, 1992, 1995, 1998, 2005; Tortell & Price, 1996). In more detailed studies, low inorganic Zn concentrations have been demonstrated to reduce the activities of key specific Zn metalloenzymes dramatically, such as carbonic anhydrase, which facilitates the acquisition of bicarbonate (Morel et al., 1994), and alkaline phosphatase, which allows phytoplankton to acquire phosphorous from organic phosphorus compounds (Shaked et al., 2006). In some regions of the ocean (e.g., areas of high nutrient and low chlorophyll) Zn addition can result in increased growth rates (Chappell et al., 2016; Coale, 1991; Franck, Bruland, Hutchins, & Brzezinski, 2003; Jakuba, Saito, Moffett, & Xu, 2012). In addition, in some cases, subtle changes in phytoplankton composition (ecosystem structure) have been observed with the addition of Zn (Crawford et al., 2003; Leblanc et al., 2005; Lohan, Crawford, Purdie, & Statham, 2005).

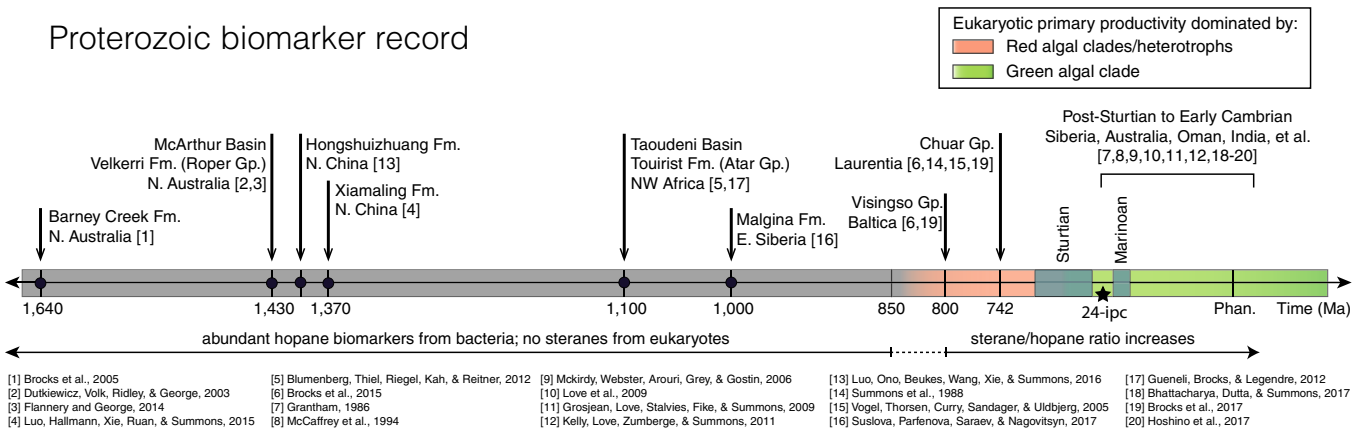


**FIGURE 1** Organic biomarker record depicting the presence/absence of eukaryotic steranes in Proterozoic organic-rich shales [Colour figure can be viewed at wileyonlinelibrary.com]

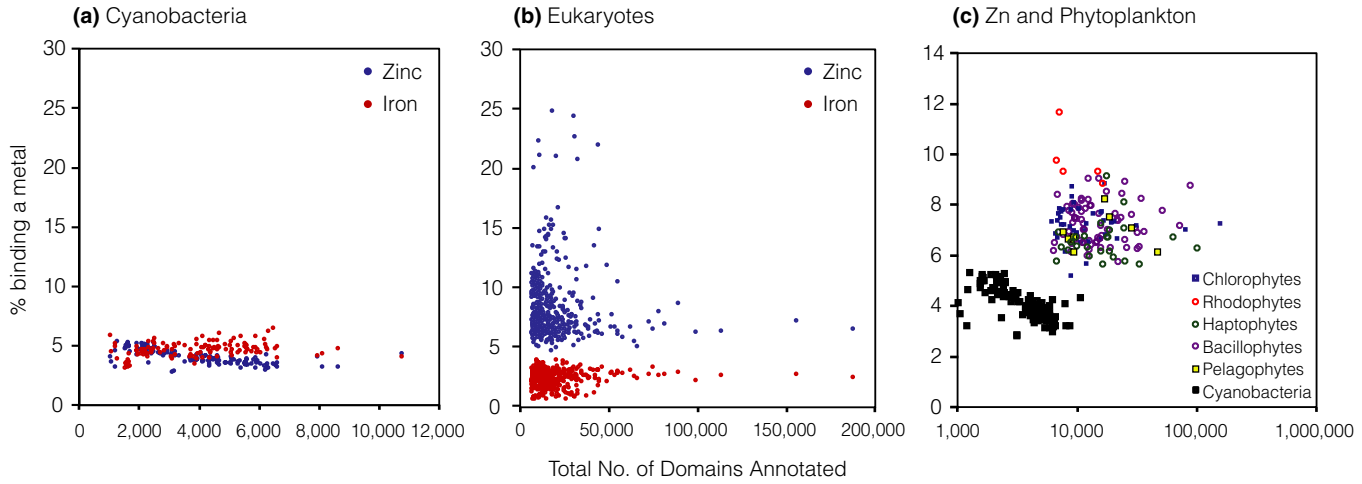


**FIGURE 2** Genome encoded metal utilization: The percentage of iron (red) and zinc (blue) binding domains compared with the total number of protein domains in discrete genomes of (a) cyanobacteria ($n$ = 123) and (b) eukaryotes ($n$ = 437). (c) Percentage of zinc-binding domains in eukaryotic and prokaryotic phytoplankton, relative to the total number of protein domains encoded by each genome [Colour figure can be viewed at wileyonlinelibrary.com]

In contrast, culture studies of cyanobacteria conducted thus far have not found Zn demands similar to that observed in eukaryotes. In culture studies the common marine cyanobacteria *Prochlorococcus* and *Synechococcus* appear not have resolvable Zn requirements, demonstrating invariant growth rates when Zn is depleted (Brand et al., 1983; Saito, Moffett, Chisholm, & Waterbury, 2002; Sunda & Huntsman, 1995). However, it has been discovered that extant cyanobacteria are not entirely devoid of Zn. For instance Zn-carbonic anhydrase metalloenzymes have been found to be expressed in cyanobacteria (Blindauer, 2008; So et al., 2004). Further, more recent culture work has highlighted the possible use of Zn in proteins involved in $PO_4^{3-}$ acquisition when subject to phosphorous deficiency (Cox & Saito, 2013)—likely linked to the expression of extracellular phosphatase in cyanobacteria (Bar-Yosef, Sukenik, Hadas, Viner-Mozzini, & Kaplan, 2010; Whitton, Grainger, Hawley, & Simon, 1991). It is important to note that with increasingly elevated ambient Zn levels, more Zn can be incorporated into cyanobacteria (Ohnemus et al., 2017). However, this high uptake may be inadvertent and it is unlikely that there had ever been markedly elevated Zn concentrations in surface waters due to Zn sorption, uptake, and scavenging. Cyanobacteria also have a higher cellular surface area to volume ratio (relative to eukaryotic cells) that facilitates higher degrees of adsorption over assimilation, such that a cyanobacteria-dominated ecosystem is in theory capable of forcing the same degree of Zn drawdown in surface waters with a much lower degree of organically incorporated Zn. During this time, iron oxide scavenging could have also significantly influenced water column Zn profiles. Therefore, although more work is required, field studies and culture work both strongly support the observation that substantially less Zn will be incorporated into biomass when cyanobacteria instead of eukaryotic phytoplankton are the dominant primary producers.

Genomic surveys of genes encoding for metal binding proteins provide an additional means to probe Zn requirements and the evolutionary history of Zn utilization. Based on predicted Zn binding proteins from whole genome sequences, high Zn requirements are observed for all major eukaryotic clades (Dupont, Butcher, Valas, Bourne, & Caetano-Anollés, 2010; Dupont, Yang, Palenik, & Bourne, 2006). In fact, our analysis with updated genomic databases (Figure 2) suggests that Zn is often the most abundant inorganic cofactor in eukaryotic enzymes across all lineages. Further, eukaryotic genomes have significantly more Zn binding proteins than prokaryotes as a percentage of the total predicted proteome (Figure 2a–b; see Appendix S1). We find that high numbers of genes for Zn binding proteins are not only found in later evolving clades that dominate modern oceans, but also in some of the earliest evolving groups of eukaryotic algae, such as rhodophytes (Figure 2c). Diverse use of Zn in eukaryotes is clearly a conserved and basal trait (Figure 2c). Although genomic data cannot be directly translated into Zn quotas, this work supports the premise that there is a fundamental difference between eukaryotic and prokaryotic Zn utilization and that this difference would have been present in early evolving eukaryotes. Contrasts in Zn usage can be linked to an abundance of nucleus-localized proteins in eukaryotes (e.g., Zn fingers and RING domains) responsible for DNA–RNA transcription and protein–protein interactions (Berg & Shi, 1996; Dupont et al., 2010; Rhodes & Klug, 1993; Twining et al., 2004). This relationship is consistent with observations from marine plankton that reveal Zn localization within the nuclei, a hallmark feature of eukaryotes (Twining & Baines, 2013; Twining, Baines, Vogt, Jonge, & Martin, 2008; Twining et al., 2003, 2004). In sum, whole-cell Zn measurements and genome-based analyses support the assertion that eukaryotic phytoplankton have significantly elevated Zn utilization relative to prokaryotic phytoplankton.

## 3 | GLOBAL ZINC ISOTOPE MASS BALANCE: ORGANIC BIOMASS, A LARGE AND ISOTOPICALLY LIGHT SINK FOR ZINC

The global mean $\delta^{66}$Zn value of modern seawater is ~0.5‰, while sources of Zn to the oceans, including riverine, aerosol, and

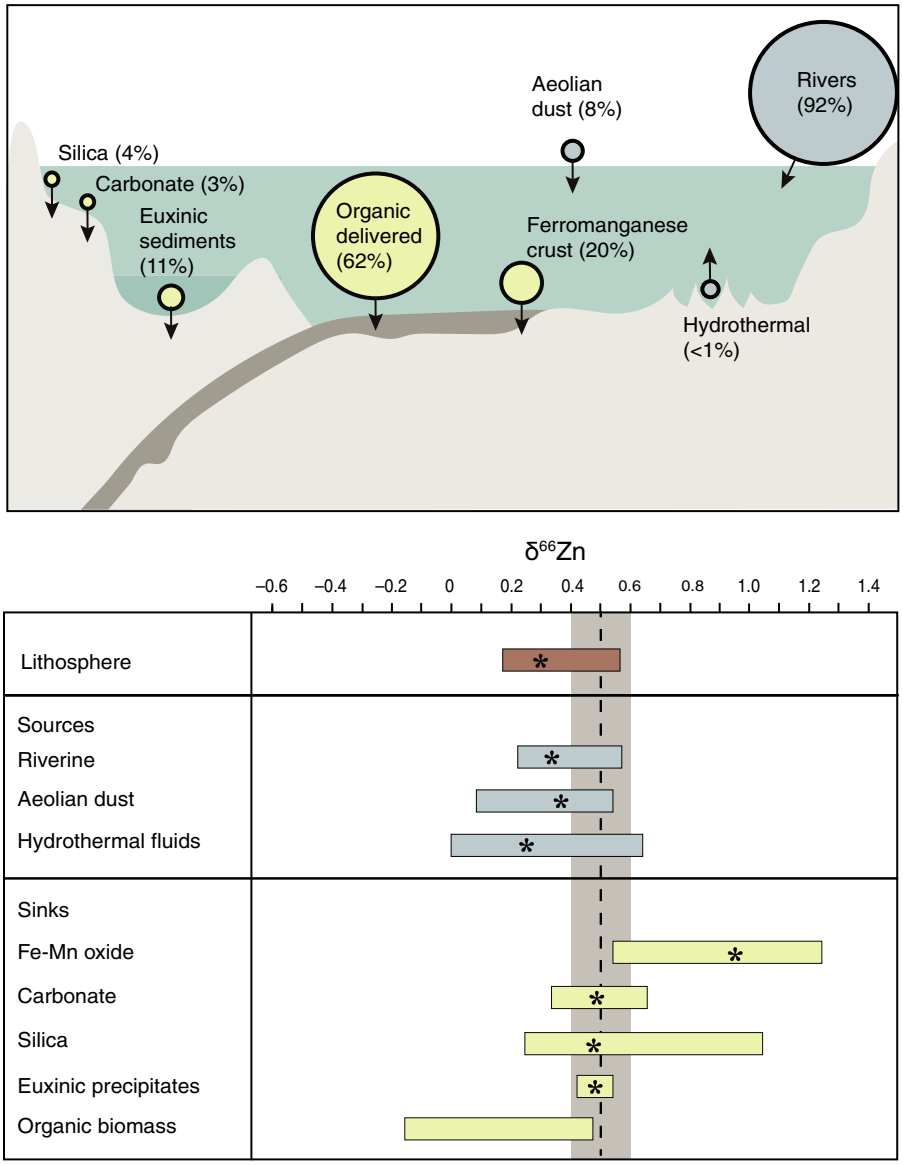


**FIGURE 3** Modern global isotopic mass balance of Zn. (Top) fluxes. (Bottom) Isotopic range. The dashed line represents mean $\delta^{66}$Zn values (0.5‰) of deep seawater, and the asterisks in bars highlight the mean $\delta^{66}$Zn values for these sources and sinks. Flux estimates in round brackets are $\times 10^8$ mol year$^{-1}$ of Zn. See Table S1 for full list of references [Colour figure can be viewed at wileyonlinelibrary.com]

hydrothermal inputs, are close to the average crustal value of ~0.3‰ (Little, Vance, Walker-Brown, & Landing, 2014). Iron and manganese oxides scavenge isotopically heavy Zn ($\Delta^{66}$Zn ~0.3 to 0.5‰) (Bryan, Dong, Wilkes, & Wasylenki, 2015; Little, Sherman, Vance, & Hein, 2014; Maréchal, Nicolas, Douchet, & Albarède, 2000; Pokrovsky, Viers, & Freydier, 2005). Carbonates appear to be unfractionated from seawater; however, isotopically heavy carbonates have been observed within the geologic record (e.g., Pichat, Douchet, & Albarède, 2003). While we do not yet understand the specific controls on Zn incorporation into carbonates (Van Dijk, De Nooijer, Wolthers, & Reichart, 2017), ab initio work suggests that the isotopic signature of Zn associated with carbonate species ought to vary with ambient pH levels (Fujii, Moynier, Blichert-Toft, & Albarède, 2014). In the most recent summary of the global isotope mass balance of Zn, the isotopically light sink was not fully resolved (Little, Vance, et al., 2014), although organic-rich continental margins have been shown to bury light Zn (Little, Vance, Mcmanus, & Severmann, 2016). Here, we build from previous work on the Zn mass balance and new data that constrain the isotopic composition of previously unidentified organic and sulfide marine export fluxes (Figure 3). We discuss each of the major Zn burial terms and propose a balanced modern Zn isotope budget (Figures 3 and 4).

Culture experiments reveal that eukaryotic phytoplankton preferentially incorporate the lighter isotopes of Zn with an isotopic fractionation ($\Delta^{66}Zn_{org\text{-}sw}$) between −0.8‰ to −0.2‰ (John & Conway, 2014; John et al., 2007). The way in which biological fractionations manifest in the oceans may depend on a variety of processes including the ambient Zn concentrations, the extent of water column consumption, and the $\delta^{66}$Zn of waters supplied to the euphotic zone. However, we have found that kerogen (the insoluble organic fraction) and bitumen (the soluble organic fraction) extracted from core-top sites across the Cariaco Basin (see methods for full extraction details) are all characterized by $\delta^{66}$Zn values that are more depleted than ambient waters, providing clear evidence that biological export sequesters isotopically depleted (light) Zn within the sediments (Figure 4). The export of light organic Zn has

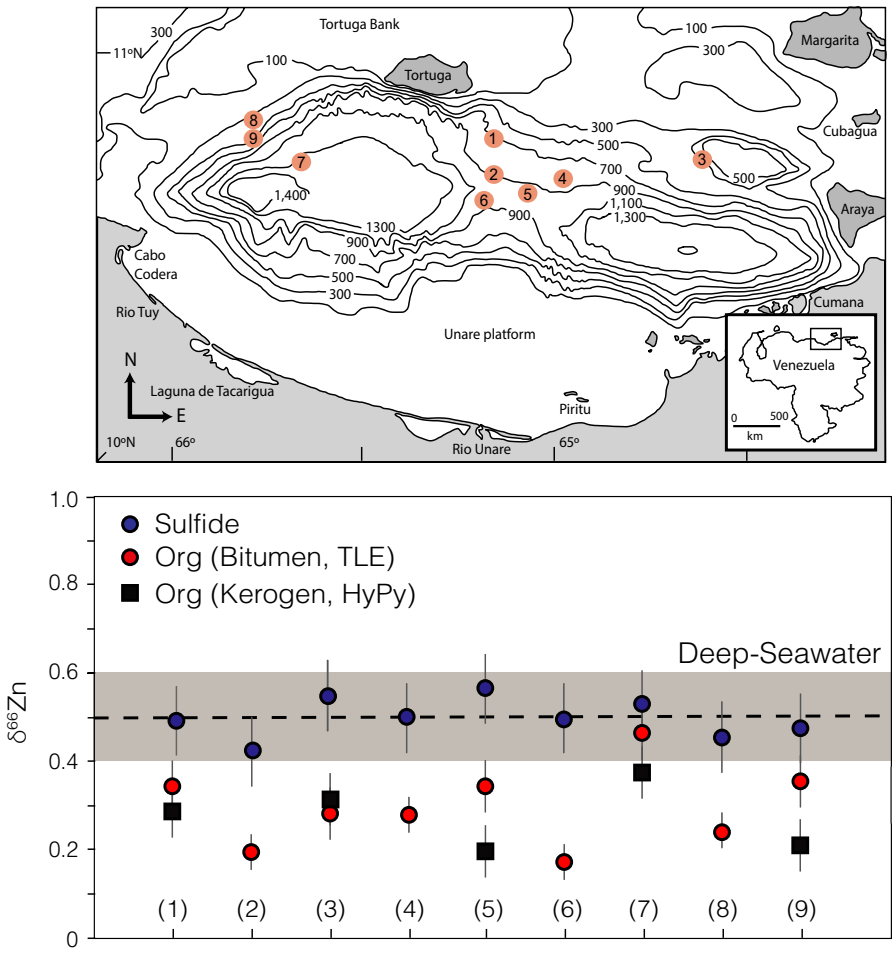


**FIGURE 4** Zn isotope data of the sulfide, bitumen (TLE), and kerogen (HyPy) fractions of euxinic core-top muds from nine sites across the Cariaco Basin. The mean value of $\delta^{66}Zn_{sulf}$ (+0.50 ± 0.07‰ 2SD, *n* = 9) accurately captures the global deep ocean water $\delta^{66}Zn$ signature (+0.50 ± 0.14‰ 2SD, *n* = 223). Vertical error bars denote external reproducibility. $\delta^{66}Zn_{org}$ values are consistently more negative than those of deep seawater [Colour figure can be viewed at wileyonlinelibrary.com]

also been suggested in other modern marine settings based on Zn isotope analyses in bulk sediments (Little et al., 2016).In a critical manner, we also provide evidence for preferential burial of isotopically light organic Zn in ancient sedimentary rocks (i.e., $\delta^{66}Zn$ values less than seawater input sources of approximately +0.33‰ (Little, Vance, et al., 2014); Figure 5b). Although the isotopic composition of organic Zn in ancient shales of low thermal maturity is variable, these $\delta^{66}Zn_{org}$ values are on average significantly lighter than the assumed input terms. Thus, the $\delta^{66}Zn_{org}$ record provides clear evidence that the organic Zn flux leads to burial of isotopically light Zn.

Profiles for $\delta^{66}Zn$ in modern marine water columns do not typically increase toward the surface despite the export of light organic Zn from seawater (Conway & John, 2014; John & Conway, 2014; Zhao, Vance, Abouchami, & De Baar, 2014). This apparent lack of an expressed biological fractionation in near-surface waters may reflect a role for Zn adsorption in controlling water column $\delta^{66}Zn$ (John & Conway, 2014; Köbberich & Vance, 2017) (Figure S1). Zinc is predominantly complexed by organic ligands, many with unknown structures, or sorbed to biological or mineralogical surfaces (Bruland, 1989; Jakuba et al., 2012; John & Conway, 2014; Lohan, Statham, & Crawford, 2002). Ligands preferentially complex the heavy isotope (Jouvin, Louvat, Juillot, Maréchal, & Benedetti, 2009; Köbberich & Vance, 2017; Marković et al., 2016), leaving the residual dissolved $Zn^{2+}$ pool isotopically light (John & Conway, 2014). It has been proposed that natural phytoplankton communities also have the ability to regulate ambient Zn concentrations in surface waters via rapid ligand production to reduce Zn toxicity, particularly where Zn concentrations are high (Lohan et al., 2005). The abundance of organic ligands has been observed to be closely linked with rates of surface productivity (John & Conway, 2014; Kozelka & Bruland, 1998; Lohan et al., 2005; Wells, Kozelka, & Bruland, 1998). The size of this organic ligand pool can be extremely dynamic, with generation and remineralization occurring on the time scale of days. Rapid oxidation of organic ligands in both surface waters and at depth releases the ligand-bound Zn back into solution (John & Conway, 2014; Lohan et al., 2005). The likelihood of any geologically meaningful ligand-bound Zn burial flux is therefore low. This assumption is consistent with our dataset, which indicates isotopically depleted $\delta^{66}Zn_{org}$ relative to sulfide bound Zn ($\delta^{66}Zn_{sulf}$) across the breadth of the geological record (see below; Figure 2). In sum, multiple processes govern the expression of Zn isotopes in surface waters, each associated with potentially large intrinsic fractionations. Water column isotopic profiles therefore express intricate spatial and temporal variability that cannot be accounted for by any single process (e.g., uptake, sorption, remineralization), and future work will no doubt continue to move forward our understanding of Zn cycling in the upper oceans. However, what is critical for our purposes is

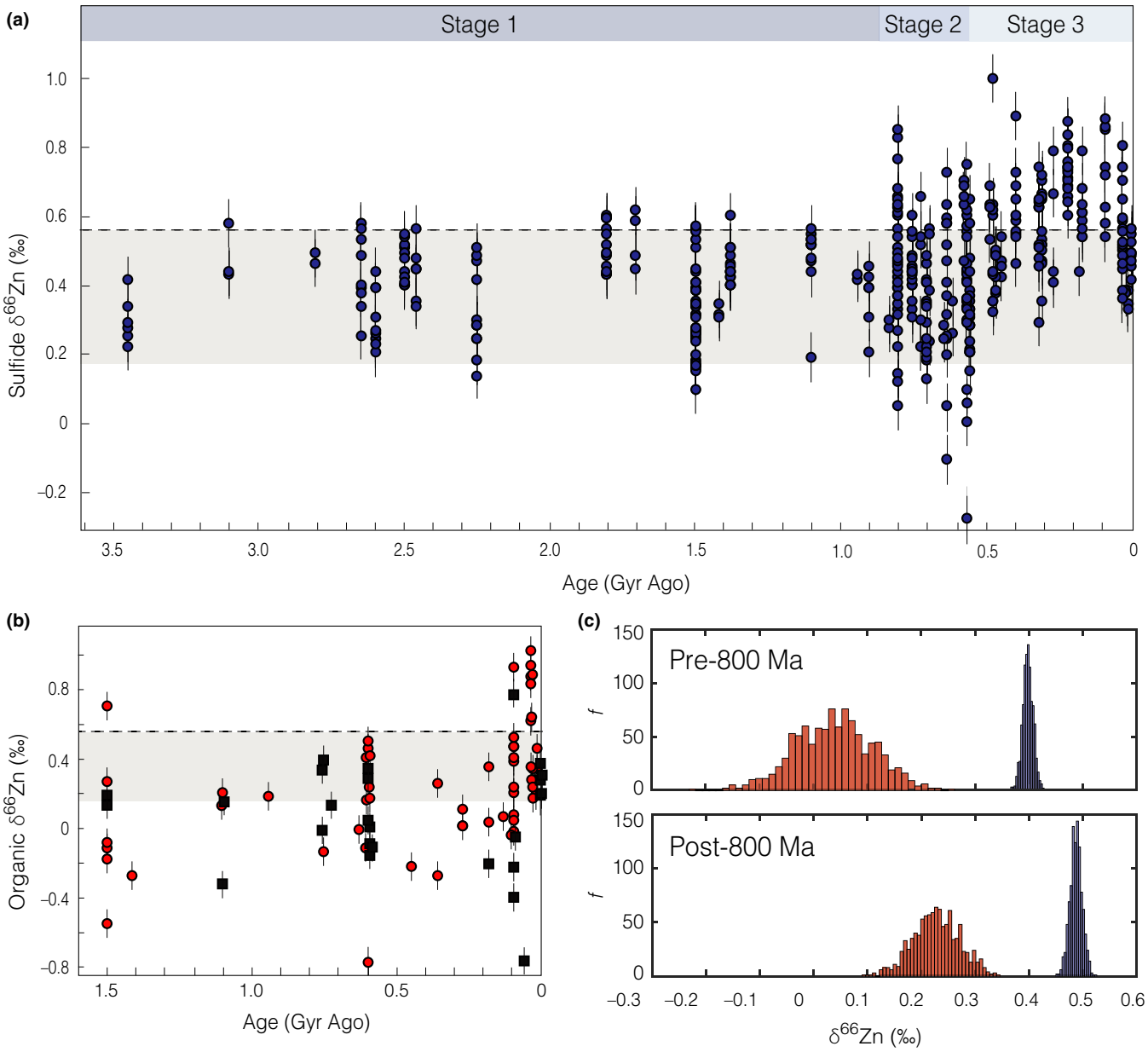


**FIGURE 5** Sedimentary Zn isotope record spanning 3.5 billion years of Earth's history. (a–b) New data from the sulfide (blue circles), bitumen (red circles) and kerogen (black squares) fractions of sulphidic black shales ($n$ = 502). Horizontal gray fields denote the crustal Zn isotopic range (32). Vertical error bars denote external reproducibility. We identify three stages within the sulfide record. Stage 1 (pre-800 Ga): sulfides express restricted values within the crustal range. Stage 2 (late Neoproterozoic): transition interval during which $\delta^{66}Zn_{sulf}$ values distinctively lighter and heavier than the crustal range are expressed, likely reflecting both the ecological rise of eukaryotes and re-organization of the global biogeochemical Zn cycle. Stage 3 (Phanerozoic): isotopically light $\delta^{66}Zn_{sulf}$ values are absent, and mean values are distinctively more positive than those of the crustal average. (c) Frequency distributions of bootstrap resampled means of sulfide (blue) and organic (bitumen and kerogen) (red) Zn isotope data pre- and post-800 Ma [Colour figure can be viewed at wileyonlinelibrary.com]

that the isotopic composition of the burial fluxes ultimately controls the mean values for global and deep-water dissolved $\delta^{66}Zn$ and that modern and ancient sedimentary organic matter (Figures 4 and 5) are isotopically depleted.

Sulfide capture is particularly important to our discussion because of our emphasis on shale-hosted isotopic data. At depths >100–300 m in the modern oceans, the isotopic composition and concentration of dissolved Zn are largely homogenous (+0.50 ± 0.14‰ 2*SD*, $n$ = 223; Bruland, 1980; Conway & John, 2014; Conway & John, 2015; Jakuba et al., 2012; John & Conway, 2014; John, Helgoe, & Townsend, 2017; Zhao et al., 2014). Hence, temporal variations in the isotopic signature of the deep-sea reservoir can therefore shed light on changes in the global biogeochemical cycling of Zn. Here, we provide new data indicating that capture of Zn in euxinic sediments can serve as a seawater archive based on analysis of sediments from the Cariaco Basin. The Cariaco Basin is permanently (rather than seasonally) euxinic (anoxic and sulfidic) and Zn precipitates out of solution either as authigenic Zn sulfides or by scavenging

during iron sulfide precipitation (Morse & Luther, 1999). Sulfides can also capture organic-delivered Zn released during biomass decay within sedimentary porewaters, a process that would drive the signature toward lighter $\delta^{66}$Zn values typical of organic matter. Zinc sulfide formation can also be associated with a negative isotope fractionation (Vance et al., 2016). However, near-quantitative Zn drawdown, due to much lower Zn concentration relative to that of $H_2S$, as is typical in sulfide-rich water columns and porewaters (e.g., Tankéré et al., 2001), is likely to mute isotope fractionation tied to aqueous Zn speciation or kinetic effects during sulfide precipitation (John, Kunzmann, Townsend, & Rosenberg, 2017; Vance et al., 2016). Consistent with muted fractionations during sulfide formation, we find that $\delta^{66}$Zn values for authigenic sulfide from core-top sites across the Cariaco Basin (+0.50 ± 0.07‰; Figure 4) are indistinguishable from the globally homogenous $\delta^{66}$Zn in the modern deep ocean (+0.50 ± 0.14‰, $n$ = 223). As Atlantic deep waters are the main source of Zn into the Cariaco Basin, these observations support that there is limited net isotopic offset from seawater during Zn sulfide burial. Building on these observations, we propose that sulfides will not be a major lever in driving changes in the isotopic composition of seawater. In sum, sulfides in black shales deposited in ancient anoxic settings can provide a robust record of dissolved $\delta^{66}$Zn values for seawater as it has evolved over geologic time.

Within this global Zn isotope mass balance framework, the burial of isotopically light Zn tied to biological uptake is the central process that can drive the global seawater $\delta^{66}$Zn to values that are more positive than the inputs (Figure 3). This framework builds from the mechanisms controlling Zn burial and all available sedimentary Zn isotope data (see below). Assuming that there is no temporal variation in the $\delta^{66}$Zn of inputs, positive shifts in mean seawater $\delta^{66}$Zn values can thus be caused by (i) an increase in the amount of isotopically light organic burial and/or (ii) a larger net isotopic fractionation for biological Zn uptake driven by greater Zn bioavailability. We find that the fractionation factor associated with organic Zn burial ($\Delta^{66}Zn_{org\text{-}diss}$) can be estimated to rule out option (2), making it possible to use Zn isotopes to quantitatively track the evolution of eukaryotic organic carbon export as a result of their significantly elevated Zn requirements.

## 4 | ZINC ISOTOPE SYSTEMATICS THROUGH TIME

We present an extensive new Zn isotope record ($n$ = 502) from a large sample set of organic-rich black shales spanning from the Archean to the present (Figure 5), with the aim of using the $\delta^{66}Zn_{sulf}$ record to track seawater evolution and organic-bound Zn to estimate the isotopic offset between organic matter and coeval seawater ($\Delta^{66}Zn_{org\text{-}sulf}$) through time. In a specific manner, these data encompass a comprehensive record of leached sulfide phases ($\delta^{66}Zn_{sulf}$) from previously examined black shales from 65 formations (Figure 5a). We focused on sulfidic shales, which have a high potential for capturing globally homogenous deep seawater values (see above). Prior to the mid-Neoproterozoic (~800 Ma), the sulfide fraction in the examined black shales shows $\delta^{66}$Zn values indistinguishable from those of the presumed input sources (mean +0.33‰, range +0.17 to +0.58‰; Figures 5, S4–S5). The first data well above assumed input values are found in the ~800 Ma Wynniatt Formation of the Shaler Supergroup in Arctic Canada ($\delta^{66}Zn_{sulf}$ > 0.9‰) (Thomson, Rainbird, Planavsky, Lyons, & Bekker, 2015) (Figure 5, S5). These positive $\delta^{66}Zn_{sulf}$ values remain prevalent throughout the late Neoproterozoic and the Phanerozoic. Variability in $\delta^{66}Zn_{sulf}$ values after ~800 Ma can be tied to shifts in either global deep water, local seawater, or varying porewater signals that overprint the global signal. Nonetheless, the onset of positive $\delta^{66}Zn_{sulf}$ values records a fundamental shift in the global Zn cycle. We propose that this shift in global Zn isotope cycling at ~800 Ma marks an increase in the burial of organic-derived Zn, principally as eukaryotic biomass, rather than changes in global redox conditions or Zn bioavailability (see Supplementary Information and below for discussion).

Oxygenation through the Neoproterozoic was likely progressive (e.g., Pogge von Strandmann et al., 2015), and this oxygenation would have reshaped the Zn cycle. Specifically, the burial of Zn associated with oxides is an important component of the modern Zn isotope budget, and this flux would have increased with ocean oxygenation. Oxide bound Zn burial was likely reduced in largely anoxic oceans. As oxide burial is associated with a positive Zn isotope effect, Zn-metal oxide burial ought to decrease rather than increase dissolved seawater $\delta^{66}$Zn values and therefore cannot explain the observed shift at ~800 Ma. In contrast, more oxic conditions would have led to a corresponding decrease in sulfide burial once sulfate burial in an increasingly well-oxygenated ocean became prevalent. Further, although the ratio of water column to porewater sulfide burial may have decreased with ocean oxygenation, Zn capture within both porewaters and euxinic water columns is likely to be near quantitative and thus any possible (intrinsic) Zn isotope fractionation during sulfide formation (e.g., Vance et al., 2016) is unlikely to be expressed.

Variations in aqueous Zn speciation may also be expected with a shift in ocean redox chemistry. Foremost, marine sulfate levels have increased dramatically throughout Earth's history tracking increasing oxygenation and ought to have increased at least transiently at around 800 Ma (Turner & Bekker, 2016). However, a rise in sulfate levels is unlikely to explain the observed isotopic trends given that Zn-sulfate complexes are weak and make-up a negligible component (<6%) of marine Zn species today (Black, Kavner, & Schauble, 2011; Fujii et al., 2014), despite marine sulfate levels that are currently at their highest point in Earth's history (Canfield & Farquhar, 2009). In addition even if present, ab initio calculations predict limited isotopic fractionation associated with the formation of Zn-sulfate complexes (Fujii, Moynier, Pons, & Albarède, 2011). Thus, ocean oxygenation is likely to have had a significant effect on the global Zn cycle, but this process is unlikely to have directly driven the observed shift to more positive $\delta^{66}Zn_{sulf}$ values in the Neoproterozoic through oxide-or sulfide burial-related controls.

The bioavailability of Zn in seawater has the potential to influence the Zn isotope fractionation associated with biological uptake. Low levels of Zn bioavailability in Proterozoic oceans were previously proposed based on thermodynamic considerations (Saito, Sigman, &

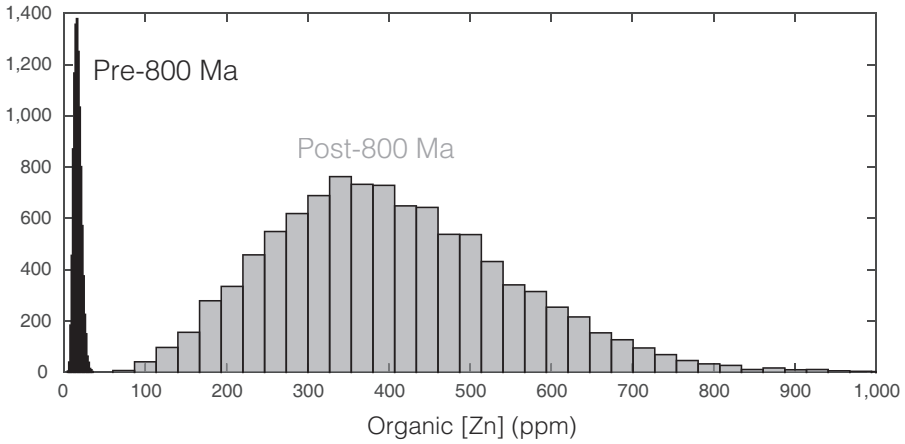


**FIGURE 6** Frequency distributions of bootstrap resampled means of organic (bitumen and kerogen) Zn abundance data, as presented in Figure 5, pre- (black) and post (gray)-800 Ma [Colour figure can be viewed at wileyonlinelibrary.com]

Morel, 2003), and low Zn bioavailability could in principle have resulted in muted $\Delta^{66}Zn_{org\text{-}sw}$ values prior to ~800 Ma. However, this model has recently been challenged based on records of appreciable sedimentary Zn enrichment during this interval (Figure S3) and thus ample supplies in seawater (Robbins et al., 2013; Scott et al., 2012). Our Zn isotope dataset supports the latter view. Specifically, we observe near constant $\Delta^{66}Zn_{org\text{-}sulf}$ values of about −0.36‰ prior to ~800 Ma (Figure 5), indicating that burial of isotopically light Zn with organic matter occurred prior to the mid-Neoproterozoic rise in $\delta^{66}Zn_{sulf}$ values. Therefore, the light Zn isotope values recorded in the organic fraction of shales indicate that the observed shift in $\delta^{66}Zn_{sulf}$ (i.e., our proxy for coeval bottom waters) is also unlikely to be linked to a shift in Zn isotope fractionation during organic matter uptake and burial. We observe a subtle shift toward smaller mean $\Delta^{66}Zn_{org\text{-}sulf}$ values after ~800 Ma from −0.36‰ to −0.26‰ (Figure 5c), which would, if anything, mute the observed increase in $\delta^{66}Zn_{sulf}$.

The observed trend in organic Zn data is unlikely to reflect a pattern of alteration, because only strata of low thermal maturity with no discernible contamination were selected for $\delta^{66}Zn_{org}$ analysis (oil window maturity or lower based on Rock-Eval pyrolysis and lipid biomarker data; see Supplementary Information). Therefore we conclude that light organic Zn was being delivered to the sediment pile through the Proterozoic, but the extent of organic-derived Zn burial was likely too low to drive seawater to significantly heavy $\delta^{66}Zn$ values prior to 800 Ma. This model is consistent with an observed jump in organic Zn concentrations in the mid-Neoproterozoic (by over an order of magnitude in terms of bootstrap resampled mean values; Figure 6).

We find that the most parsimonious explanation for the observed mid-Neoproterozoic-Phanerozoic rise in marine $\delta^{66}Zn$ is an increase in organic-derived Zn burial, given evidence for the nearly constant $\Delta^{66}Zn_{org\text{-}sulf}$ values, an expected decrease in deep ocean $\delta^{66}Zn$ with ocean oxygenation via removal of $^{66}Zn$ onto metal oxides, and a smaller sulfide sink for Zn. We propose that this transition was most likely caused by both a higher Zn demand following the rise of eukaryotes to ecological dominance in phase with an overall increase in total global productivity. We find in our Zn isotope mass balance that an increase in organic carbon burial alone is insufficient to account for

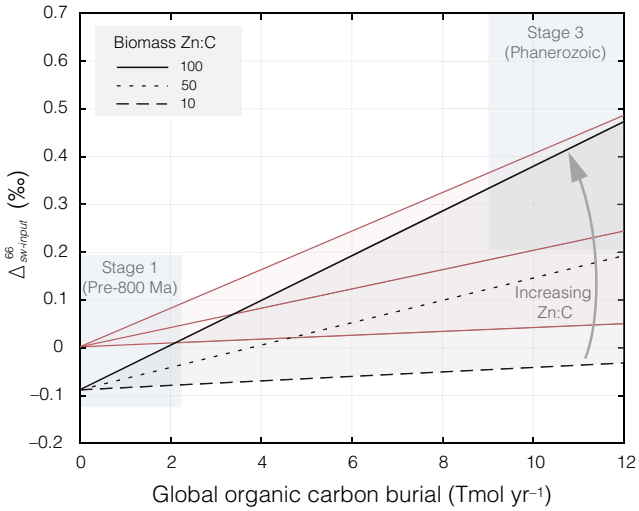


**FIGURE 7** Global Zn isotope mass balance for a pre- and post-800 Ma ocean, illustrating deviations in the Zn isotopic composition of seawater away from mean source input values (vertical axis), with given changes in (1) organic carbon burial (horizontal axis) and (2) the Zn/C ratio of organic biomass being exported (dashed and solid lines). Black lines represent modern oxic removal flux ($1.7 \times 10^8$ mol $yr^{-1}$), and red represents calculations for a pervasively reducing ocean in which there is negligible oxic burial. We adopt a biological isotope fractionation from seawater ($\Delta^{66}Zn_{org\text{-}sw}$) of −0.5‰, and a riverine input flux of $13 \times 10^8$ moles $yr^{-1}$. Our modeling suggests that that the Zn isotope composition of seawater is largely insensitive to a system largely characterized by prokaryotic cells (Zn/C ratio of ~10). This model suggests that much larger Zn/C ratios of ~100, typical of eukaryotic phytoplankton, are required for any ocean system to achieve $\delta^{66}Zn$ values that are 0.5–0.7‰ greater than the source mean, a feature of post-800 Ma seawater. An increase in organic-derived Zn burial across the mid-Neoproterozoic suggests a fundamental restructuring of global marine ecosystem structures, toward a more eukaryote-rich system in which there is more extensive biological Zn utilization (Figure S2) [Colour figure can be viewed at wileyonlinelibrary.com]

the positive Zn isotope values observed in post-800 Ma sediments if buried with the Zn/C ratio we observe for pre-800 Ma sedimentary organic matter (Figure 7). Rather, we find that increases in marine organic Zn/C are essential to drive the observed rise in seawater

$\delta^{66}$Zn (Figure 7). This framework is consistent with the observed late Neoproterozoic to Phanerozoic increase in organic Zn concentrations (Figure 6). We propose that the observed rise in sedimentary organic Zn/C is likely linked to a larger eukaryotic contribution (with an elevated Zn/C ratio) to exported marine biomass. Moreover, our first markedly positive Zn isotope values appear around 800 Ma, but additional work in the Neoproterozoic and Phanerozoic is needed to determine if the Neoproterozoic Zn cycle oscillated between typical mid-Proterozoic and late Neoproterozoic/Phanerozoic states as opposed to a single state change.

## 5 | CONCLUSION

Given fossil evidence for eukaryote emergence at > ~1700 Ma (Butterfield, 2015; Knoll, 2014; Parfrey, Lahr, Knoll, & Katz, 2011), our Zn records provide support for a long (billon-year) lag before their rise to ecological prominence at ~800 Ma, which is consistent with the earliest robust finding of detectable sterane compounds in thermally well-preserved sedimentary rocks (Brocks et al., 2017). This sterane biomarker signal was attributed to mainly unicellular heterotrophic protists, as gauged from the unusual $C_{27}$ sterane carbon number dominance (Brocks et al., 2017), but substantial contributions from eukaryotic phytoplankton (in particular from red algal clades) could produce similar sterane patterns (Kodner, Pearson, Summons, & Knoll, 2008) and account for some appreciable sterane/hopane ratios (0.003–0.42 reported for a small 720–820 Ma sample set) (Brocks et al., 2017). In addition, the Zn record provides an opportunity to evaluate the impact that the first abundant eukaryotic export productivity may have had on Neoproterozoic climatic and carbon cycle perturbations. For instance, the shift in ecosystem structure recorded in our isotopic data occurred almost 80 million years before the onset of the "Snowball Earth" events challenges previous suggestions that algal proliferation was intimately and directly linked with the onset of glaciation (Feulner et al., 2015; Tziperman et al., 2011). At the same time, the increase in eukaryote contribution to primary productivity coincided with a dramatic shift toward more dynamic carbon isotope values in marine carbonates following more than a billion years of relative $\delta^{13}$C stability, and just prior to the first appearance of microfossils for testate amoebae (eukaryotic heterotrophs) (Porter & Knoll, 2000), marking the end of an extended biogeochemical stasis that prevailed in the preceding "boring billion". While establishing the cause and effect relationships behind these observations via more detailed Neoproterozoic records remains important for future research, the Zn isotope record nevertheless suggests that the proliferation of eukaryotes in the oceans was closely coupled with the onset of dynamic environmental and biogeochemical evolution during the mid-Neoproterozoic.

## ACKNOWLEDGMENTS

The authors acknowledge funding from the NSF FESD Program (TL, GL) and the NASA Astrobiology Institute under Cooperative Agreement No. NNA15BB03A issued through the Science Mission Directorate (TL, CD, CR, GL, NP, etc.). We are extremely grateful to Andy Knoll, Larry Peterson and Christopher Junium for providing samples for this study.

## ORCID

*Terry T. Isson* http://orcid.org/0000-0002-1040-0230
*Alan D. Rooney* http://orcid.org/0000-0002-5023-2606
*Eva E. Stueeken* http://orcid.org/0000-0001-6861-2490

## REFERENCES

Anderson, M., Morel, F., & Guillard, R. (1978). Growth limitation of a coastal diatom by low zinc ion activity. *Nature*, *276*, 70–71. https://doi.org/10.1038/276070a0

Bar-Yosef, Y., Sukenik, A., Hadas, O., Viner-Mozzini, Y., & Kaplan, A. (2010). Enslavement in the water body by toxic Aphanizomenon ovalisporum, inducing alkaline phosphatase in phytoplanktons. *Current Biology*, *20*, 1557–1561. https://doi.org/10.1016/j.cub.2010.07.032

Berg, J. M., & Shi, Y. (1996). The galvanization of biology: A growing appreciation for the roles of zinc. *Science*, *271*, 1081–1085. https://doi.org/10.1126/science.271.5252.1081

Bhattacharya, S., Dutta, S., & Summons, R. E. (2017). A distinctive biomarker assemblage in an Infracambrian oil and source rock from western India: Molecular signatures of eukaryotic sterols and prokaryotic carotenoids. *Precambrian Research*, *290*, 101–112. https://doi.org/10.1016/j.precamres.2016.12.013

Black, J. R., Kavner, A., & Schauble, E. A. (2011). Calculation of equilibrium stable isotope partition function ratios for aqueous zinc complexes and metallic zinc. *Geochimica et Cosmochimica Acta*, *75*, 769–783. https://doi.org/10.1016/j.gca.2010.11.019

Blindauer, C. A. (2008). Zinc-handling in cyanobacteria: An update. *Chemistry and Biodiversity*, *5*, 1990–2013. https://doi.org/10.1002/cbdv.200890183

Blumenberg, M., Thiel, V., Riegel, W., Kah, L. C., & Reitner, J. (2012). Biomarkers of black shales formed by microbial mats, Late Mesoproterozoic (1.1 Ga) Taoudeni Basin, Mauritania. *Precambrian Research*, *196*, 113–127. https://doi.org/10.1016/j.precamres.2011.11.010

Brand, L. E., Sunda, W. G., & Guillard, R. R. (1983). Limitation of marine phytoplankton reproductive rates by zinc, manganese, and iron. *Limnology and Oceanography*, *28*, 1182–1198. https://doi.org/10.4319/lo.1983.28.6.1182

Brocks, J. J., Jarrett, A. J., Sirantoine, E., Hallmann, C., Hoshino, Y., & Liyanage, T. (2017). The rise of algae in Cryogenian oceans and the emergence of animals. *Nature*, *548*, 578. https://doi.org/10.1038/nature23457

Brocks, J. J., Jarrett, A. J., Sirantoine, E., Kenig, F., Moczydlowska, M., Porter, S., & Hope, J. (2015). Early sponges and toxic protists: Possible sources of cryostane, an age diagnostic biomarker antedating Sturtian Snowball Earth. *Geobiology*, *14*, 129–149.

Brocks, J. J., Love, G. D., Summons, R. E., Knoll, A. H., Logan, G. A., & Bowden, S. A. (2005). Biomarker evidence for green and purple sulphur bacteria in a stratified Palaeoproterozoic sea. *Nature*, *437*, 866–870. https://doi.org/10.1038/nature04068

Bruland, K. W. (1980). Oceanographic distributions of cadmium, zinc, nickel, and copper in the North Pacific. *Earth and Planetary Science Letters*, *47*, 176–198. https://doi.org/10.1016/0012-821X(80)90035-7

Bruland, K. W. (1989). Complexation of zinc by natural organic ligands in the central North Pacific. *Limnology and Oceanography*, *34*, 269–285. https://doi.org/10.4319/lo.1989.34.2.0269

Bryan, A. L., Dong, S., Wilkes, E. B., & Wasylenki, L. E. (2015). Zinc isotope fractionation during adsorption onto Mn oxyhydroxide at low and high ionic strength. *Geochimica et Cosmochimica Acta*, *157*, 182–197. https://doi.org/10.1016/j.gca.2015.01.026

Butterfield, N. J. (2015). Early evolution of the Eukaryota. *Palaeontology*, *58*, 5–17. https://doi.org/10.1111/pala.12139

Canfield, D. E., & Farquhar, J. (2009). Animal evolution, bioturbation, and the sulfate concentration of the oceans. *Proceedings of the National Academy of Sciences of the United States of America*, *106*, 8123–8127. https://doi.org/10.1073/pnas.0902037106

Chappell, P. D., Vedmati, J., Selph, K. E., Cyr, H. A., Jenkins, B. D., Landry, M. R., & Moffett, J. W. (2016). Preferential depletion of zinc within Costa Rica Upwelling Dome creates conditions for zinc co-limitation of primary production. *Journal of Plankton Research*, *38*, 244–255. https://doi.org/10.1093/plankt/fbw018

Coale, K. H. (1991). Effects of iron, manganese, copper, and zinc enrichments on productivity and biomass in the subarctic Pacific. *Limnology and Oceanography*, *36*, 1851–1864. https://doi.org/10.4319/lo.1991.36.8.1851

Conway, T. M., & John, S. G. (2014). The biogeochemical cycling of zinc and zinc isotopes in the North Atlantic Ocean. *Global Biogeochemical Cycles*, *28*, 1111–1128. https://doi.org/10.1002/2014GB004862

Conway, T. M., & John, S. G. (2015). The cycling of iron, zinc and cadmium in the North East Pacific Ocean – Insights from stable isotopes. *Geochimica et Cosmochimica Acta*, *164*, 262–283. https://doi.org/10.1016/j.gca.2015.05.023

Cox, A. D., & Saito, M. A. (2013). Proteomic responses of oceanic Synechococcus WH8102 to phosphate and zinc scarcity and cadmium additions. *Frontiers in Microbiology*, *4*, 387.

Crawford, D., Lipsen, M., Purdie, D., Lohan, M., Statham, P., Whitney, F., … Peterson, T. (2003). Influence of zinc and iron enrichments on phytoplankton growth in the northeastern subarctic Pacific. *Limnology and Oceanography*, *48*, 1583–1600. https://doi.org/10.4319/lo.2003.48.4.1583

Dupont, C. L., Butcher, A., Valas, R. E., Bourne, P. E., & Caetano-Anollés, G. (2010). History of biological metal utilization inferred through phylogenomic analysis of protein structures. *Proceedings of the National Academy of Sciences of the United States of America*, *107*, 10567–10572. https://doi.org/10.1073/pnas.0912491107

Dupont, C. L., Yang, S., Palenik, B., & Bourne, P. E. (2006). Modern proteomes contain putative imprints of ancient shifts in trace metal geochemistry. *Proceedings of the National Academy of Sciences of the United States of America*, *103*, 17822–17827. https://doi.org/10.1073/pnas.0605798103

Dutkiewicz, A., Volk, H., Ridley, J., & George, S. (2003). Biomarkers, brines, and oil in the Mesoproterozoic, Roper Superbasin, Australia. *Geology*, *31*, 981–984. https://doi.org/10.1130/G19754.1

Ellwood, M. J., & Hunter, K. A. (2000). The incorporation of zinc and iron into the frustule of the marine diatom *Thalassiosira pseudonana*. *Limnology and Oceanography*, *45*, 1517–1524. https://doi.org/10.4319/lo.2000.45.7.1517

Falkowski, P. G., Katz, M. E., Knoll, A. H., Quigg, A., Raven, J. A., Schofield, O., & Taylor, F. J. (2004). The evolution of modern eukaryotic phytoplankton. *Science*, *305*, 354–360. https://doi.org/10.1126/science.1095964

Feulner, G., Hallmann, C., & Kienert, H. (2015). Snowball cooling after algal rise. *Nature Geoscience*, *8*, 659–662. https://doi.org/10.1038/ngeo2523

Flannery, E. N., & George, S. C. (2014). Assessing the syngeneity and indigeneity of hydrocarbons in the- 1.4 Ga Velkerri Formation, McArthur Basin, using slice experiments. *Organic Geochemistry*, *77*, 115–125. https://doi.org/10.1016/j.orggeochem.2014.10.008

Franck, V. M., Bruland, K. W., Hutchins, D. A., & Brzezinski, M. A. (2003). Iron and zinc effects on silicic acid and nitrate uptake kinetics in three high-nutrient, low-chlorophyll (HNLC) regions. *Marine Ecology Progress Series*, *252*, 15–33. https://doi.org/10.3354/meps252015

French, K. L., Hallmann, C., Hope, J. M., Schoon, P. L., Zumberge, J. A., Hoshino, Y., … Summons, R. E. (2015). Reappraisal of hydrocarbon biomarkers in Archean rocks. *Proceedings of the National Academy of Sciences of the United States of America*, *112*, 5915–5920. https://doi.org/10.1073/pnas.1419563112

Fujii, T., Moynier, F., Blichert-Toft, J., & Albarède, F. (2014). Density functional theory estimation of isotope fractionation of Fe, Ni, Cu, and Zn among species relevant to geochemical and biological environments. *Geochimica et Cosmochimica Acta*, *140*, 553–576. https://doi.org/10.1016/j.gca.2014.05.051

Fujii, T., Moynier, F., Pons, M.-L., & Albarède, F. (2011). The origin of Zn isotope fractionation in sulfides. *Geochimica et Cosmochimica Acta*, *75*, 7632–7643. https://doi.org/10.1016/j.gca.2011.09.036

Grantham, P. (1986). The occurence of unusual C 27 and C 29 sterane predominances in two types of Oman crude oil. *Organic Geochemistry*, *9*, 1–10. https://doi.org/10.1016/0146-6380(86)90077-X

Grosjean, E., Love, G., Stalvies, C., Fike, D., & Summons, R. (2009). Origin of petroleum in the Neoproterozoic–Cambrian South Oman salt basin. *Organic Geochemistry*, *40*, 87–110. https://doi.org/10.1016/j.orggeochem.2008.09.011

Gueneli, N., Brocks, J., & Legendre, E. (2012). *1.1 Billion-years-old biomarkers from a microbial mat*. Mineralogical Magazine A, 1565.

Hoshino, Y., Poshibaeva, A., Meredith, W., Snape, C., Poshibaev, V., Versteegh, G. J., … Neumann, M. (2017). Cryogenian evolution of stigmasteroid biosynthesis. *Science Advances*, *3*, e1700887. https://doi.org/10.1126/sciadv.1700887

Jakuba, R. W., Saito, M. A., Moffett, J. W., & Xu, Y. (2012). Dissolved zinc in the subarctic North Pacific and Bering Sea: Its distribution, speciation, and importance to primary producers. *Global Biogeochemical Cycles*, *26*, 1–15.

John, S. G., & Conway, T. M. (2014). A role for scavenging in the marine biogeochemical cycling of zinc and zinc isotopes. *Earth and Planetary Science Letters*, *394*, 159–167. https://doi.org/10.1016/j.epsl.2014.02.053

John, S. G., Geis, R. W., Saito, M. A., & Boyle, E. A. (2007). Zinc isotope fractionation during high-affinity and low-affinity zinc transport by the marine diatom *Thalassiosira oceanica*. *Limnology and Oceanography*, *52*, 2710–2714. https://doi.org/10.4319/lo.2007.52.6.2710

John, S. G., Helgoe, J., & Townsend, E. (2017). Biogeochemical cycling of Zn and Cd and their stable isotopes in the Eastern Tropical South Pacific. *Marine Chemistry*, *201*, 256–262.

John, S. G., Kunzmann, M., Townsend, E. J., & Rosenberg, A. D. (2017). Zinc and cadmium stable isotopes in the geological record: A case study from the post-snowball Earth Nuccaleena cap dolostone. *Palaeogeography, Palaeoclimatology, Palaeoecology*, *466*, 202–208. https://doi.org/10.1016/j.palaeo.2016.11.003

Jouvin, D., Louvat, P., Juillot, F., Maréchal, C. N., & Benedetti, M. F. (2009). Zinc isotopic fractionation: Why organic matters. *Environmental Science and Technology*, *43*, 5747–5754. https://doi.org/10.1021/es803012e

Kelly, A. E., Love, G. D., Zumberge, J. E., & Summons, R. E. (2011). Hydrocarbon biomarkers of Neoproterozoic to Lower Cambrian oils from eastern Siberia. *Organic Geochemistry*, *42*, 640–654. https://doi.org/10.1016/j.orggeochem.2011.03.028

Knoll, A. H. (2014). Paleobiological perspectives on early eukaryotic evolution. *Cold Spring Harbor Perspectives in Biology*, *6*, a016121. https://doi.org/10.1101/cshperspect.a016121

Knoll, A. H., Javaux, E. J., Hewitt, D., & Cohen, P. (2006). Eukaryotic organisms in Proterozoic oceans. *Philosophical Transactions of the Royal Society B: Biological Sciences*, *361*, 1023–1038. https://doi.org/10.1098/rstb.2006.1843

Köbberich, M., & Vance, D. (2017). Kinetic control on Zn isotope signatures recorded in marine diatoms. *Geochimica et Cosmochimica Acta*, *210*, 97–113. https://doi.org/10.1016/j.gca.2017.04.014

Kodner, R. B., Pearson, A., Summons, R. E., & Knoll, A. H. (2008). Sterols in red and green algae: Quantification, phylogeny, and relevance for the interpretation of geologic steranes. *Geobiology*, *6*, 411–420. https://doi.org/10.1111/j.1472-4669.2008.00167.x

Kozelka, P. B., & Bruland, K. W. (1998). Chemical speciation of dissolved Cu, Zn, Cd, Pb in Narragansett Bay, Rhode Island. *Marine Chemistry*, *60*, 267–282. https://doi.org/10.1016/S0304-4203(97)00107-2

Leblanc, K., Hare, C., Boyd, P., Bruland, K., Sohst, B., Pickmere, S., … Hutchins, D. (2005). Fe and Zn effects on the Si cycle and diatom community structure in two contrasting high and low-silicate HNLC areas. *Deep Sea Research Part I: Oceanographic Research Papers*, *52*, 1842–1864. https://doi.org/10.1016/j.dsr.2005.06.005

Little, S. H., Sherman, D. M., Vance, D., & Hein, J. R. (2014). Molecular controls on Cu and Zn isotopic fractionation in Fe–Mn crusts. *Earth and Planetary Science Letters*, *396*, 213–222. https://doi.org/10.1016/j.epsl.2014.04.021

Little, S. H., Vance, D., Mcmanus, J., & Severmann, S. (2016). Key role of continental margin sediments in the oceanic mass balance of Zn and Zn isotopes. *Geology*, *G37493*, 37491.

Little, S. H., Vance, D., Walker-Brown, C., & Landing, W. M. (2014). The oceanic mass balance of copper and zinc isotopes, investigated by analysis of their inputs, and outputs to ferromanganese oxide sediments. *Geochimica et Cosmochimica Acta*, *125*, 673–693. https://doi.org/10.1016/j.gca.2013.07.046

Lohan, M. C., Crawford, D. W., Purdie, D. A., & Statham, P. J. (2005). Iron and zinc enrichments in the northeastern subarctic Pacific: Ligand production and zinc availability in response to phytoplankton growth. *Limnology and Oceanography*, *50*, 1427. https://doi.org/10.4319/lo.2005.50.5.1427

Lohan, M. C., Statham, P. J., & Crawford, D. W. (2002). Total dissolved zinc in the upper water column of the subarctic North East Pacific. *Deep Sea Research Part II: Topical Studies in Oceanography*, *49*, 5793–5808. https://doi.org/10.1016/S0967-0645(02)00215-1

Love, G. D., Grosjean, E., Stalvies, C., Fike, D. A., Grotzinger, J. P., Bradley, A. S., … Summons, R. E. (2009). Fossil steroids record the appearance of Demospongiae during the Cryogenian period. *Nature*, *457*, 718–721. https://doi.org/10.1038/nature07673

Luo, G., Hallmann, C., Xie, S., Ruan, X., & Summons, R. E. (2015). Comparative microbial diversity and redox environments of black shale and stromatolite facies in the Mesoproterozoic Xiamaling Formation. *Geochimica et Cosmochimica Acta*, *151*, 150–167. https://doi.org/10.1016/j.gca.2014.12.022

Luo, G., Ono, S., Beukes, N. J., Wang, D. T., Xie, S., & Summons, R. E. (2016). Rapid oxygenation of Earth's atmosphere 2.33 billion years ago. *Science Advances*, *2*, e1600134. https://doi.org/10.1126/sciadv.1600134

Maréchal, C. N., Nicolas, E., Douchet, C., & Albarède, F. (2000). Abundance of zinc isotopes as a marine biogeochemical tracer. *Geochemistry, Geophysics, Geosystems*, *1*, 5.

Marković, T., Manzoor, S., Humphreys-Williams, E., Kirk, G. J., Vilar, R., & Weiss, D. J. (2016). Experimental determination of zinc isotope fractionation in complexes with the phytosiderophore 2′-deoxymugeneic acid (DMA) and its structural analogues, and implications for plant uptake mechanisms. *Environmental Science and Technology*, *51*, 98–107.

Mccaffrey, M. A., Moldowan, J. M., Lipton, P. A., Summons, R. E., Peters, K. E., Jeganathan, A., & Watt, D. S. (1994). Paleoenvironmental implications of novel C 30 steranes in Precambrian to Cenozoic age petroleum and bitumen. *Geochimica et Cosmochimica Acta*, *58*, 529–532. https://doi.org/10.1016/0016-7037(94)90481-2

Mckirdy, D. M., Webster, L. J., Arouri, K. R., Grey, K., & Gostin, V. A. (2006). Contrasting sterane signatures in Neoproterozoic marine rocks of Australia before and after the Acraman asteroid impact. *Organic Geochemistry*, *37*, 189–207. https://doi.org/10.1016/j.orggeochem.2005.09.005

Morel, F. M. M., Reinfelder, J. R., Roberts, S. B., Chamberlain, C. P., Lee, J. G., & Yee, D. (1994). Zinc and carbon co-limitation of marine phytoplankton. *Nature*, *369*, 740–742. https://doi.org/10.1038/369740a0

Morse, J., & Luther, G. (1999). Chemical influences on trace metal-sulfide interactions in anoxic sediments. *Geochimica et Cosmochimica Acta*, *63*, 3373–3378. https://doi.org/10.1016/S0016-7037(99)00258-6

Nuester, J., Vogt, S., Newville, M., Kustka, A. B., & Twining, B. S. (2012). The unique biogeochemical signature of the marine diazotroph Trichodesmium. *Environmental Bioinorganic Chemistry of Aquatic Microbial Organisms*, *164*, 1–15.

Ohnemus, D. C., Rauschenberg, S., Cutter, G. A., Fitzsimmons, J. N., Sherrell, R. M., & Twining, B. S. (2017). Elevated trace metal content of prokaryotic communities associated with marine oxygen deficient zones. *Limnology and Oceanography*, *62*, 3–25. https://doi.org/10.1002/lno.10363

Parfrey, L. W., Lahr, D. J., Knoll, A. H., & Katz, L. A. (2011). Estimating the timing of early eukaryotic diversification with multigene molecular clocks. *Proceedings of the National Academy of Sciences of the United States of America*, *108*, 13624–13629. https://doi.org/10.1073/pnas.1110633108

Pichat, S., Douchet, C., & Albarède, F. (2003). Zinc isotope variations in deep-sea carbonates from the eastern equatorial Pacific over the last 175 ka. *Earth and Planetary Science Letters*, *210*, 167–178. https://doi.org/10.1016/S0012-821X(03)00106-7

Pogge von Strandmann, P. A., Stüeken, E. E., Elliott, T., Poulton, S. W., Dehler, C. M., Canfield, D. E., & Catling, D. C. (2015). Selenium isotope evidence for progressive oxidation of the Neoproterozoic biosphere. *Nature Communications*, *6*, 10157.

Pokrovsky, O. S., Viers, J., & Freydier, R. (2005). Zinc stable isotope fractionation during its adsorption on oxides and hydroxides. *Journal of Colloid and Interface Science*, *291*, 192–200. https://doi.org/10.1016/j.jcis.2005.04.079

Porter, S. M., & Knoll, A. H. (2000). Testate amoebae in the Neoproterozoic Era: Evidence from vase-shaped microfossils in the Chuar Group, Grand Canyon. *Paleobiology*, *26*, 360–385. https://doi.org/10.1666/0094-8373(2000)026<0360:TAITNE>2.0.CO;2

Quigg, A., Irwin, A. J., & Finkel, Z. V. (2011). Evolutionary inheritance of elemental stoichiometry in phytoplankton. *Proceedings of the Royal Society of London B: Biological Sciences*, *278*, 526–534. https://doi.org/10.1098/rspb.2010.1356

Rhodes, D., & Klug, A. (1993). Zinc fingers. *Scientific American*, *268*, 56–65. https://doi.org/10.1038/scientificamerican0293-56

Robbins, L. J., Lalonde, S. V., Saito, M. A., Planavsky, N. J., Mloszewska, A. M., Pecoits, E., … Konhauser, K. O. (2013). Authigenic iron oxide proxies for marine zinc over geological time and implications for eukaryotic metallome evolution. *Geobiology*, *11*, 295–306. https://doi.org/10.1111/gbi.12036

Saito, M. A., Moffett, J. W., Chisholm, S. W., & Waterbury, J. B. (2002). Cobalt limitation and uptake in Prochlorococcus. *Limnology and Oceanography*, *47*, 1629–1636. https://doi.org/10.4319/lo.2002.47.6.1629

Saito, M. A., Sigman, D. M., & Morel, F. M. (2003). The bioinorganic chemistry of the ancient ocean: The co-evolution of cyanobacterial metal requirements and biogeochemical cycles at the Archean–Proterozoic boundary? *Inorganica Chimica Acta*, *356*, 308–318. https://doi.org/10.1016/S0020-1693(03)00442-0

Schulz, K. G., Zondervan, I., Gerringa, L., Timmermans, K., Veldhuis, M., & Riebesell, U. (2004). Effect of trace metal availability on coccolithophorid calcification. *Nature*, *430*, 673–676. https://doi.org/10.1038/nature02631

Scott, C., Planavsky, N. J., Dupont, C. L., Kendall, B., Gill, B. C., Robbins, L. J., … Lyons, T. W. (2012). Bioavailability of zinc in marine systems through time. *Nature Geoscience*, *6*, 125–128.

Shaked, Y., Xu, Y., Leblanc, K., & Morel, F. M. (2006). Zinc availability and alkaline phosphatase activity in *Emiliania huxleyi*: Implications for Zn-P co-limitation in the ocean. *Limnology and Oceanography*, *51*, 299–309. https://doi.org/10.4319/lo.2006.51.1.0299

So, A. K.-C., Espie, G. S., Williams, E. B., Shively, J. M., Heinhorst, S., & Cannon, G. C. (2004). A novel evolutionary lineage of carbonic anhydrase (ε class) is a component of the carboxysome shell. *Journal of Bacteriology*, *186*, 623–630. https://doi.org/10.1128/JB.186.3.623-630.2004

Summons, R. E., Brassell, S. C., Eglinton, G., Evans, E., Horodyski, R. J., Robinson, N., & Ward, D. M. (1988). Distinctive hydrocarbon biomarkers from fossiliferous sediment of the Late Proterozoic Walcott Member, Chuar Group, Grand Canyon, Arizona. *Geochimica et Cosmochimica Acta*, *52*, 2625–2637. https://doi.org/10.1016/0016-7037(88)90031-2

Sunda, W. G., & Huntsman, S. A. (1992). Feedback interactions between zinc and phytoplankton in seawater. *Limnology and Oceanography*, *37*, 25–40. https://doi.org/10.4319/lo.1992.37.1.0025

Sunda, W. G., & Huntsman, S. A. (1995). Cobalt and zinc interreplacement in marine phytoplankton: Biological and geochemical implications. *Limnology and Oceanography*, *40*, 1404–1417. https://doi.org/10.4319/lo.1995.40.8.1404

Sunda, W. G., & Huntsman, S. A. (1998). Processes regulating cellular metal accumulation and physiological effects: Phytoplankton as model systems. *Science of the Total Environment*, *219*, 165–181. https://doi.org/10.1016/S0048-9697(98)00226-5

Sunda, W. G., & Huntsman, S. A. (2005). Effect of $CO_2$ supply and demand on zinc uptake and growth limitation in a coastal diatom. *Limnology and Oceanography*, *50*, 1181–1192. https://doi.org/10.4319/lo.2005.50.4.1181

Suslova, E., Parfenova, T., Saraev, S., & Nagovitsyn, K. (2017). Organic geochemistry of rocks of the Mesoproterozoic Malgin Formation and their depositional environments (southeastern Siberian Platform). *Russian Geology and Geophysics*, *58*, 516–528. https://doi.org/10.1016/j.rgg.2016.09.027

Tankéré, S., Muller, F., Burton, J., Statham, P., Guieu, C., & Martin, J.-M. (2001). Trace metal distributions in shelf waters of the northwestern Black Sea. *Continental Shelf Research*, *21*, 1501–1532. https://doi.org/10.1016/S0278-4343(01)00013-9

Thomson, D., Rainbird, R. H., Planavsky, N., Lyons, T. W., & Bekker, A. (2015). Chemostratigraphy of the Shaler Supergroup, Victoria Island, NW Canada: A record of ocean composition prior to the Cryogenian glaciations. *Precambrian Research*, *263*, 232–245. https://doi.org/10.1016/j.precamres.2015.02.007

Tortell, P. D., & Price, N. M. (1996). Cadmium toxicity and zinc limitation in centric diatoms of the genus Thalassiosira. *Marine Ecology Progress Series*, *138*, 245–254. https://doi.org/10.3354/meps138245

Turner, E., & Bekker, A. (2016). Thick sulfate evaporite accumulations marking a mid-Neoproterozoic oxygenation event (Ten Stone Formation, Northwest Territories, Canada). *Geological Society of America Bulletin*, *128*, 203–222.

Twining, B. S., & Baines, S. B. (2013). The trace metal composition of marine phytoplankton. *Annual Review of Marine Science*, *5*, 191–215. https://doi.org/10.1146/annurev-marine-121211-172322

Twining, B. S., Baines, S. B., Bozard, J. B., Vogt, S., Walker, E. A., & Nelson, D. M. (2011). Metal quotas of plankton in the equatorial Pacific Ocean. *Deep Sea Research Part II: Topical Studies in Oceanography*, *58*, 325–341. https://doi.org/10.1016/j.dsr2.2010.08.018

Twining, B. S., Baines, S. B., & Fisher, N. S. (2004). Element stoichiometries of individual plankton cells collected during the Southern Ocean Iron Experiment(SOFeX). *Limnology and Oceanography*, *49*, 2115–2128. https://doi.org/10.4319/lo.2004.49.6.2115

Twining, B. S., Baines, S. B., Fisher, N. S., Maser, J., Vogt, S., Jacobsen, C., … Sañudo-Wilhelmy, S. A. (2003). Quantifying trace elements in individual aquatic protist cells with a synchrotron X-ray fluorescence microprobe. *Analytical Chemistry*, *75*, 3806–3816. https://doi.org/10.1021/ac034227z

Twining, B. S., Baines, S. B., Vogt, S., Jonge, D., & Martin, D. (2008). Exploring ocean biogeochemistry by single-cell microprobe analysis of protist elemental composition. *Journal of Eukaryotic Microbiology*, *55*, 151–162. https://doi.org/10.1111/j.1550-7408.2008.00320.x

Tziperman, E., Halevy, I., Johnston, D. T., Knoll, A. H., & Schrag, D. P. (2011). Biologically induced initiation of Neoproterozoic snowball-Earth events. *Proceedings of the National Academy of Sciences of the United States of America*, *108*, 15091–15096. https://doi.org/10.1073/pnas.1016361108

Van Dijk, I., De Nooijer, L. J., Wolthers, M., & Reichart, G.-J. (2017). Impacts of pH and [CO3 2–] on the incorporation of Zn in foraminiferal calcite. *Geochimica et Cosmochimica Acta*, *197*, 263–277. https://doi.org/10.1016/j.gca.2016.10.031

Vance, D., Little, S. H., Archer, C., Cameron, V., Andersen, M. B., Rijkenberg, M. J., & Lyons, T. W. (2016). The oceanic budgets of nickel and zinc isotopes: The importance of sulfidic environments as illustrated by the Black Sea. *Philosophical Transactions of the Royal Society A: Mathematical, Physical and Engineering Sciences*, *374*, 20150294. https://doi.org/10.1098/rsta.2015.0294

Vogel, I., Thorsen, P., Curry, A., Sandager, P., & Uldbjerg, N. (2005). Biomarkers for the prediction of preterm delivery. *Acta obstetricia et gynecologica Scandinavica*, *84*, 516–525. https://doi.org/10.1111/j.0001-6349.2005.00771.x

Wells, M. L., Kozelka, P. B., & Bruland, K. W. (1998). The complexation of dissolved 'Cu, Zn, Cd and Pb by soluble and colloidal organic matter in Narragansett Bay, RI. *Marine Chemistry*, *62*, 203–217. https://doi.org/10.1016/S0304-4203(98)00041-3

Whitton, B., Grainger, S., Hawley, G., & Simon, J. (1991). Cell-bound and extracellular phosphatase activities of cyanobacterial isolates. *Microbial Ecology*, *21*, 85–98. https://doi.org/10.1007/BF02539146

Zhang, S., Wang, X., Wang, H., Bjerrum, C. J., Hammarlund, E. U., Costa, M. M., … Canfield, D. E. (2016). Sufficient oxygen for animal respiration 1,400 million years ago. *Proceedings of the National Academy of Sciences of the United States of America*, *113*, 1731–1736. https://doi.org/10.1073/pnas.1523449113

Zhao, Y., Vance, D., Abouchami, W., & De Baar, H. (2014). Biogeochemical cycling of zinc and its isotopes in the Southern Ocean. *Geochimica et Cosmochimica Acta*, *125*, 653–672. https://doi.org/10.1016/j.gca.2013.07.045

Zhu, S., Zhu, M., Knoll, A. H., Yin, Z., Zhao, F., Sun, S., … Liu, H. (2016). Decimetre-scale multicellular eukaryotes from the 1.56-billion-year-old Gaoyuzhuang Formation in North China. *Nature Communications*, *7*, 11500. https://doi.org/10.1038/ncomms11500

## SUPPORTING INFORMATION

Additional supporting information may be found online in the Supporting Information section at the end of the article.

**How to cite this article:** Isson TT, Love GD, Dupont CL, et al. Tracking the rise of eukaryotes to ecological dominance with zinc isotopes. *Geobiology*. 2018;16:341–352. https://doi.org/10.1111/gbi.12289